


SHORT COMMUNICATION

Open Access



# Quantitative [ $^{99m}\text{Tc}$ ]Tc-MDP SPECT/CT correlated with [ $^{18}\text{F}$ ]NaF PET/CT for bone metastases in patients with prostate cancer

Kenichi Tanaka<sup>1†</sup>, Takashi Norikane<sup>1†</sup>, Katsuya Mitamura<sup>1</sup>, Yuka Yamamoto<sup>1\*</sup> , Yukito Maeda<sup>2</sup>, Kengo Fujimoto<sup>1</sup>, Yasukage Takami<sup>1</sup>, Mariko Ishimura<sup>1</sup>, Hanae Arai-Okuda<sup>1</sup>, Yoichiro Tohi<sup>3</sup>, Nobuyuki Kudomi<sup>4</sup>, Mikio Sugimoto<sup>3</sup> and Yoshihiro Nishiyama<sup>1</sup>

<sup>†</sup>Kenichi Tanaka and Takashi Norikane contributed equally to this work

\*Correspondence: yamamoto.yuka@kagawa-u.ac.jp

<sup>1</sup> Department of Radiology, Faculty of Medicine, Kagawa University, 1750-1 Ikenobe, Miki-cho, Kita-gun, Kagawa 761-0793, Japan

<sup>2</sup> Department of Clinical Radiology, Kagawa University Hospital, Miki-cho, Kagawa, Japan

<sup>3</sup> Department of Urology, Faculty of Medicine, Kagawa University, Miki-cho, Kagawa, Japan

<sup>4</sup> Department of Medical Physics, Faculty of Medicine, Kagawa University, Miki-cho, Kagawa, Japan

## Abstract

**Background:** The purpose of the present study was to elucidate the correlation between standardized uptake value (SUV) and volume-based parameters measured by quantitative [ $^{99m}\text{Tc}$ ]Tc-methylene diphosphonate (MDP) single photon emission computed tomography (SPECT)/CT and [ $^{18}\text{F}$ ]-sodium fluoride ([ $^{18}\text{F}$ ]NaF) positron emission tomography (PET)/CT in the assessment of bone metastases in patients with prostate cancer.

**Methods:** The study included 26 male prostate cancer patients with confirmed or suspected bone metastases who underwent both [ $^{99m}\text{Tc}$ ]Tc-MDP SPECT/CT and [ $^{18}\text{F}$ ]NaF PET/CT studies. Skeletal lesions visible on both SPECT/CT and PET/CT were classified as benign or metastases. The maximum SUV (SUVmax), peak SUV (SUVpeak), mean SUV (SUVmean), metabolic bone volume (MBV), and total bone uptake (TBU) were calculated for every lesion showing abnormal uptake.

**Results:** A total of 202 skeletal lesions (147 benign and 55 metastases) were detected in the 26 patients. Strong significant correlations were noted between SPECT/CT and PET/CT for the SUV- and volume-based parameters (all  $P < 0.001$ ). The SUVmax, SUVpeak, SUVmean, and TBU values obtained with SPECT/CT were significantly lower than the corresponding values obtained with PET/CT (all  $P < 0.001$ ). The MBV in SPECT/CT was significantly higher than that in PET/CT ( $P < 0.001$ ). All SUV- and volume-based parameters obtained with both SPECT/CT and PET/CT for metastatic lesions were significantly higher than the corresponding parameters for benign lesions ( $P$  values from 0.036 to  $< 0.001$ ).

**Conclusions:** These preliminary results demonstrate that the SUV- and volume-based parameters for bone uptake obtained with quantitative SPECT/CT and PET/CT are strongly correlated in patients with prostate cancer. The SUV parameters obtained with SPECT/CT were significantly lower than those obtained with PET/CT, whereas the uptake volume obtained with SPECT/CT was significantly higher than that obtained with PET/CT.

**Keywords:** SPECT, PET, SUV, Bone metastases, Prostate cancer

## Background

In prostate cancer, the most common malignancy in men, bone scintigraphy is mainly used for assessment of high-risk patients, in whom the extent of bone metastases has been reported to be an independent prognostic factor [1, 2]. Single photon emission computed tomography (SPECT) with  $^{99m}\text{Tc}$ -labeled diphosphonates, such as [ $^{99m}\text{Tc}$ ]Tc-methylene diphosphonate (MDP) is used to assess bone metastases from prostate cancer. Although positron emission tomography (PET) with [ $^{18}\text{F}$ ]-sodium fluoride ([ $^{18}\text{F}$ ]NaF) is a more sensitive method than SPECT with  $^{99m}\text{Tc}$ -labeled diphosphonates for detecting bone metastases [3, 4], it is not widely used because of high cost and limited availability.

SPECT has traditionally been used in a non-quantitative manner; namely, images are interpreted using relative intensity values instead of absolute values of radiotracer concentration [5]. However, in recent years, the wide acceptance of integrated SPECT/CT scanners and the development of iterative reconstruction algorithms have enabled the clinical use of quantitative SPECT as well as PET [6]. The most commonly used semiquantitative PET parameter is the standardized uptake value (SUV). Owing to its simplicity, the maximum SUV (SUVmax) inside a lesion is mainly used to clinically represent the intensity of radioactivity within the lesion. Nowadays, volume-based parameters such as metabolic tumor volume and total lesion glycolysis have also proven to be helpful for assessments.

[ $^{18}\text{F}$ ]NaF PET/CT has very good accuracy for the diagnosis of bone metastases from prostate cancer [3, 4, 7]. However, it is not a routine modality. Moreover, although recent developments in SPECT/CT technology enable it to be used to calculate the SUV, it has not been fully compared with PET/CT as the gold standard. Thus, there is a need to standardize the evaluation and interpretation of SPECT/CT and PET/CT findings, especially in the assessment of therapeutic response. Only a single study has previously reported a direct comparison between bone SPECT/CT and [ $^{18}\text{F}$ ]NaF PET/CT using SUV-based parameters, not volume-based parameters, for measuring metastatic bone uptake [4]. This prompted us to investigate the correlation between SUV- and volume-based parameters measured by quantitative [ $^{99m}\text{Tc}$ ]Tc-MDP SPECT/CT and [ $^{18}\text{F}$ ]NaF PET/CT to assess bone metastases in patients with prostate cancer.

## Methods

### Patients

We conducted a retrospective analysis of prospectively collected data. The prospective study consisted of 48 consecutive prostate cancer patients with confirmed or suspected bone metastases who underwent [ $^{18}\text{F}$ ]NaF PET/CT between November 2018 and May 2021. All patients provided written informed consent, and the study protocol was approved by our institutional ethical review committee. Among these patients, 26 male patients (mean age, 72.0 years; age range, 56–89 years) were selected for this retrospective analysis. Eligible patients had undergone both [ $^{99m}\text{Tc}$ ]Tc-MDP SPECT/CT and [ $^{18}\text{F}$ ]NaF PET/CT studies within 2 months. Fifteen patients were newly diagnosed with high-risk prostate cancer, and the remaining 11 were suspected of showing recurrence or progression later in the course of the disease. The median interval between the [ $^{99m}\text{Tc}$ ]Tc-MDP SPECT/CT and [ $^{18}\text{F}$ ]NaF PET/CT scans was 8 days (range, 1–50 days). This

retrospective data collection was compliant with our institutional ethical review committee, which waived the requirement for informed consent.

#### **[<sup>99m</sup>Tc]Tc-MDP SPECT/CT imaging**

At 210 min after intravenous injection of [<sup>99m</sup>Tc]Tc-MDP (740 MBq), SPECT scans of the entire axial skeleton were obtained using two Symbia T16 SPECT/CT scanners (Siemens Healthcare, Erlangen, Germany) with the following parameters: low-energy high-resolution collimators, 180 projections over 360° with 8 s/step, 128 × 128 matrix, 4.8 × 4.8 mm pixel size, and 4.8 mm slice thickness. Unenhanced low-dose CT data from the same area were used for attenuation correction and image fusion. SPECT data were reconstructed using a three-dimensional (3D) ordered-subset expectation–maximization (OSEM) algorithm with 15 iterations, six subsets incorporating correction with resolution recovery, scatter correction, and an 11-mm Gaussian filter.

#### **[<sup>18</sup>F]NaF PET/CT imaging**

All acquisitions were performed using a Biograph mCT 64-slice PET/CT scanner (Siemens Healthcare; Erlangen, Germany). Emission data were obtained 90 min after intravenous injection of [<sup>18</sup>F]NaF (5 MBq/kg) from the knee to the skull (2 min per bed position). Unenhanced low-dose CT data from the same area were used for attenuation correction and image fusion. PET data were reconstructed in a 256 × 256 matrix with a pixel size of 3.18 × 3.18 mm and slice thickness of 5.0 mm using a fully 3D OSEM algorithm with two iterations, 21 subsets incorporating correction with a point-spread function and time-of-flight model, scatter correction, and a 5-mm Gaussian filter.

#### **Image analysis**

Skeletal lesions visible on both SPECT/CT and PET/CT examinations were interpreted. On the basis of the corresponding morphologic findings on the CT images of SPECT/CT and PET/CT [8], skeletal lesions with abnormal uptake were classified as benign or metastases by the consensus of a board-certified nuclear medicine physician and a board-certified radiologist. The patients' medical records were reviewed to obtain the final diagnosis of equivocal lesions.

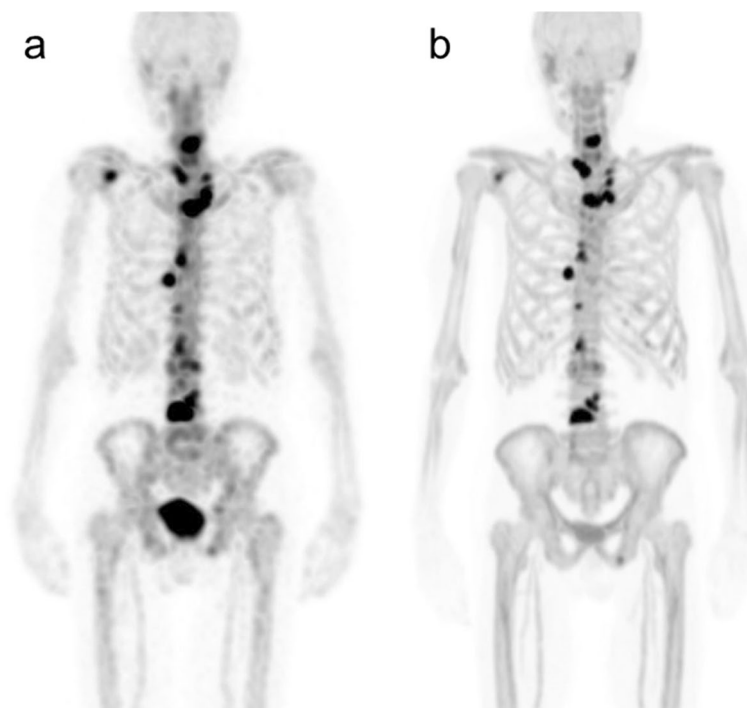
The SUV- and volume-based analyses using SPECT/CT and PET/CT were performed by a board-certified nuclear medicine physician using GI-BONE, a commercially available software package (AZE, Tokyo, Japan), and Syngo.via (Siemens Healthcare, Erlangen, Germany), respectively. The volume of interest (VOI) of the contour of the identified skeletal lesion was placed using 3D reconstructed images. A threshold was selected by visual inspection to best fit the contour of the abnormal uptake. The SUV<sub>max</sub>, peak SUV (SUV<sub>peak</sub>), defined as the mean concentration of activity within a 1-cm<sup>3</sup> spherical VOI centered on the highest voxel within the lesion, mean SUV (SUV<sub>mean</sub>), metabolic bone volume (MBV), defined as lesion volume with uptake, and total bone uptake (TBU), calculated as SUV<sub>mean</sub> × MBV, were calculated for every lesion showing abnormal uptake.

#### **Statistical analysis**

Data were analyzed using SPSS statistical software (version 28; IBM). Spearman's rank correlation coefficients were used to determine the degree of correlation between

**Table 1** Location and CT findings of 147 benign skeletal lesions identified using SPECT/CT or PET/CT

| Location       | Findings (n)   |
|----------------|--|
| Facial bones   | Sinusitis (6), dental disease (12)   |
| Cervical spine | Osteophytes (12), osteoarthritis (12)  |
| Thoracic spine | Osteophytes (23), osteoarthritis (1)   |
| Lumbar spine   | Osteophytes (22), osteoarthritis (12), fracture (5)  |
| Pelvic bones   | Osteoarthritis (3), avulsion injury (1)  |
| Thoracic cage  | Arthritic changes at the acromioclavicular (19) and sternoclavicular (1) joints, fracture (14), postoperative change (1) |
| Long bones     | Subchondral cyst (3)   |

**Fig. 1**  $^{99m}\text{Tc}$ Tc-MDP SPECT (a) and  $^{18}\text{F}$ NaF PET (b) maximum intensity projection images of an 89-year-old male with prostate cancer showing multiple bone metastases

SPECT and PET parameters. The Wilcoxon signed-rank test was used to compare the differences between SPECT and PET parameters. Differences between benign and metastatic lesions were analyzed using the Mann–Whitney  $U$ -test. Differences were considered statistically significant at  $P$  values less than 0.05.

## Results

A total of 202 skeletal lesions, including 147 benign and 55 metastases, were detected in 26 patients. Table 1 shows the CT findings of lesions identified as benign on SPECT/CT or PET/CT images with abnormal uptake. Typical SPECT and PET images are shown in Fig. 1. The median SUV threshold used for segmentation was 60% (range, 10%–80%) of the SUVmax in SPECT and 40% (range, 10%–70%) of the SUVmax in PET.

There were strong and statistically significant correlations between SPECT/CT and PET/CT parameters in SUVmax (Fig. 2a,  $\rho=0.764$ ,  $P<0.001$ ), SUVpeak (Fig. 2b,  $\rho=0.838$ ,  $P<0.001$ ), SUVmean (Fig. 2c,  $\rho=0.679$ ,  $P<0.001$ ), MBV (Fig. 2d,  $\rho=0.807$ ,  $P<0.001$ ), and TBU (Fig. 2e,  $\rho=0.874$ ,  $P<0.001$ ).

Table 2 shows the SPECT/CT and PET/CT parameters for all skeletal lesions. The SUVmax, SUVpeak, SUVmean, and TBU were all significantly lower in SPECT/CT than in PET/CT (all  $P<0.001$ ). In contrast, the MBV in SPECT/CT was significantly higher than that in PET/CT ( $P<0.001$ ).

Table 3 shows the results of SPECT/CT and PET/CT parameters for benign and metastatic lesions. For SPECT/CT, the SUVmax ( $P<0.001$ ), SUVpeak ( $P<0.001$ ), SUVmean ( $P=0.005$ ), MBV ( $P=0.002$ ), and TBU ( $P=0.002$ ) of metastatic lesions were significantly higher than those of benign lesions. For PET/CT, the SUVmax ( $P<0.001$ ), SUVpeak ( $P<0.001$ ), SUVmean ( $P<0.001$ ), MBV ( $P=0.036$ ), and TBU ( $P=0.002$ ) of metastatic lesions were also significantly higher than those of benign lesions.

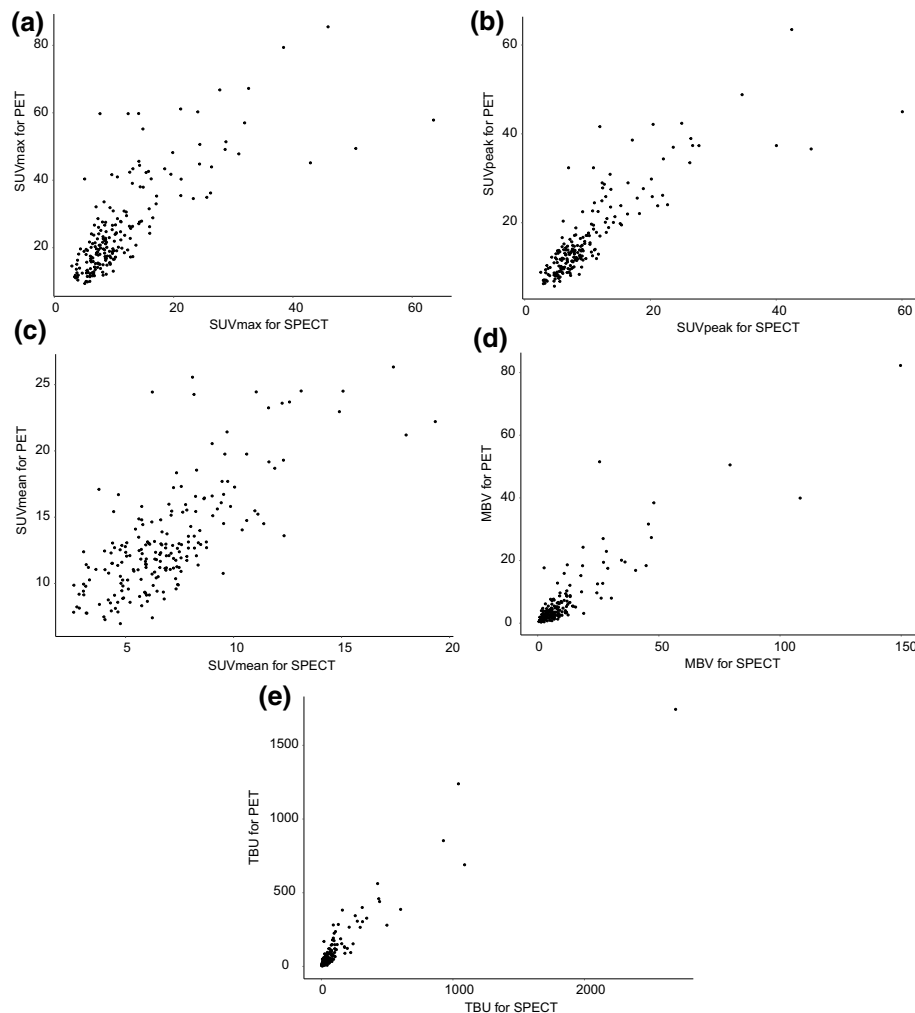


**Fig. 2** Scatter plots showing the correlation between SPECT and PET parameters in SUVmax (a) ( $\rho=0.764$ ,  $P<0.001$ ), SUVpeak (b) ( $\rho=0.838$ ,  $P<0.001$ ), SUVmean (c) ( $\rho=0.679$ ,  $P<0.001$ ), MBV (d) ( $\rho=0.807$ ,  $P<0.001$ ), and TBU (e) ( $\rho=0.874$ ,  $P<0.001$ )

**Table 2** Relationship between SPECT and PET parameters for all skeletal lesions in patients with prostate cancer

|         | SPECT               | PET                 | P value |
|---------|---------------------|---------------------|---------|
| SUVmax  | 8.66 (6.69–12.67)   | 20.50 (15.87–29.76) | <0.001  |
| SUVpeak | 7.85 (5.88–10.99)   | 13.25 (10.05–18.85) | <0.001  |
| SUVmean | 6.55 (5.01–8.04)    | 12.31 (10.41–14.82) | <0.001  |
| MBV     | 5.24 (2.65–9.98)    | 3.02 (1.66–6.10)    | <0.001  |
| TBU     | 34.20 (13.95–75.27) | 36.00 (17.71–85.82) | <0.001  |

Data are presented in terms of the median (IQR) values

SUV Standardized uptake value, SUVmax Maximum SUV, SUVpeak Peak SUV, SUVmean Mean SUV, MBV Metabolic bone volume, TBU Total bone uptake

**Table 3** Relationship between benign and metastatic lesions in terms of SPECT and PET parameters in patients with prostate cancer

|         | SPECT               |                      |         | PET                 |                      |         |
|---------|---------------------|----------------------|---------|---------------------|----------------------|---------|
|         | Benign              | Metastatic           | P value | Benign              | Metastatic           | P value |
| SUVmax  | 8.49 (6.45–10.45)   | 13.08 (7.25–24.40)   | <0.001  | 19.04 (15.28–24.73) | 32.99 (20.30–45.16)  | <0.001  |
| SUVpeak | 7.58 (5.65–9.28)    | 11.68 (6.23–20.29)   | <0.001  | 12.25 (9.68–15.14)  | 20.36 (13.60–30.90)  | <0.001  |
| SUVmean | 6.35 (4.91–7.48)    | 7.58 (5.06–10.99)    | 0.005   | 11.74 (9.92–13.03)  | 15.42 (12.45–19.76)  | <0.001  |
| MBV     | 4.62 (2.41–8.22)    | 8.48 (3.11–15.66)    | 0.002   | 2.63 (1.52–5.12)    | 3.95 (1.87–10.02)    | 0.036   |
| TBU     | 28.25 (13.07–63.06) | 52.23 (17.47–176.62) | 0.002   | 31.23 (16.94–66.51) | 48.18 (24.58–187.31) | 0.002   |

Data are presented in terms of the median (IQR) values

SUV Standardized uptake value, SUVmax Maximum SUV, SUVpeak Peak SUV, SUVmean Mean SUV, MBV Metabolic bone volume, TBU Total bone uptake

## Discussion

This study assessed the correlations of SUV- and volume-based parameters obtained using quantitative [ $^{99m}\text{Tc}$ ]Tc-MDP SPECT/CT and [ $^{18}\text{F}$ ]NaF PET/CT in the evaluation of bone metastases in patients with prostate cancer. The findings indicated that SUV- and volume-based parameters obtained using SPECT/CT and PET/CT were strongly correlated.

Even-Sapir et al. qualitatively compared the detection of bone metastases using [ $^{99m}\text{Tc}$ ]Tc-MDP SPECT and [ $^{18}\text{F}$ ]NaF PET in 44 patients with high-risk prostate cancer and showed that [ $^{18}\text{F}$ ]NaF PET was more sensitive than [ $^{99m}\text{Tc}$ ]Tc-MDP SPECT [3]. PET shows high sensitivity and resolution, allowing highly accurate whole-body screening of metastases [9]; however, it is expensive and not widely used as a clinical imaging technique for this purpose. In contrast, high-quality SPECT algorithms have recently enabled the clinical use of quantitative SPECT assessments. This prompted us to perform a quantitative analysis to compare SPECT and PET.

Only one direct comparative study has evaluated the correlations between SUV measurements obtained with bone SPECT/CT and [ $^{18}\text{F}$ ]NaF PET/CT for metastatic and benign bone uptake [4]. The authors of that study evaluated the correlations between parameters obtained using [ $^{99m}\text{Tc}$ ]Tc-hydroxyethylene (HDP) SPECT/CT and [ $^{18}\text{F}$ ]NaF PET/CT in bone metastases from breast and prostate cancer and demonstrated strong correlations of SUV parameters between SPECT and PET [4], consistent with the results of the present study. In the present study, the volume-based parameters of the

two methods were also strongly correlated. To the best of our knowledge, this is the first direct comparative study to report volume-based parameters using bone SPECT/CT and [ $^{18}\text{F}$ ]NaF PET/CT.

Schirrmeyer et al. reported that [ $^{18}\text{F}$ ]NaF PET was found to be more sensitive and accurate compared with [ $^{99\text{m}}\text{Tc}$ ]Tc-MDP bone scintigraphy for the detection of osteoblastic and osteolytic metastases in patients with breast cancer [10]. To our knowledge, there are no studies quantitatively comparing [ $^{18}\text{F}$ ]NaF PET/CT and bone SPECT/CT for osteolytic bone metastases. Yen et al. evaluated the diagnostic usefulness of [ $^{18}\text{F}$ ]NaF PET/CT relative to [ $^{99\text{m}}\text{Tc}$ ]Tc-MDP whole-body planar bone scintigraphy with no CT in detecting metastatic hepatocellular carcinoma bone lesions that are predominantly osteolytic in nature, and showed that [ $^{18}\text{F}$ ]NaF PET/CT has significantly better sensitivity and specificity [11]. Araz et al. reported that [ $^{18}\text{F}$ ]NaF PET/CT could detect both osteolytic and osteoblastic metastases as well as bone marrow involvement, and that small lesions were better visualized due to the advantages of greater spatial resolution and better image quality when compared with  $^{99\text{m}}\text{Tc}$ -labeled whole-body bone scan [12]. Another study by Cook et al. suggested that semi-quantitative [ $^{18}\text{F}$ ]NaF PET data may be useful as imaging biomarkers for monitoring treatment response in bone metastases following  $^{223}\text{Ra}$ -chloride treatment [13]. Further studies comparing the use of [ $^{18}\text{F}$ ]NaF PET/CT and bone SPECT/CT for assessment not only osteoblastic bone metastases, but also osteolytic bone metastases, are required.

In this study, the SUV parameters obtained with SPECT/CT were significantly lower than those obtained with PET/CT, which is consistent with a previous report [4]. A previous report indicated that the differences in SUV between the two methods were larger for smaller lesions. Thus, some differences were caused by the different spatial resolutions of SPECT and PET scanners [4]: because of the lower spatial resolution, underestimation of the SUV attributable to the partial-volume effect is more significant in SPECT than in PET [4, 5]. Blood protein binding interferes with the extraction of  $^{99\text{m}}\text{Tc}$ -labeled diphosphonates but does not affect the extraction of [ $^{18}\text{F}$ ]NaF [14]. Thus, the uptake of [ $^{18}\text{F}$ ]NaF was approximately twofold higher and its blood clearance was significantly faster than that of  $^{99\text{m}}\text{Tc}$ -labeled diphosphonates used in bone scintigraphy, resulting in an increased bone-to-background ratio [15]. Similarly, in this study, the median values of SUV parameters in PET were approximately twice those in SPECT. In contrast, the MBV, defined as the lesion volume with uptake, of SPECT was significantly higher than that of PET in this study. This may be due to the selection of a threshold by visual inspection to best fit the contour of abnormal uptake. Gamma-camera SPECT systems have poorer spatial resolution than PET systems [16, 17]. Umeda et al. identified a cut-off SUV<sub>max</sub> of 7.0 to assess the bone metastatic burden using [ $^{99\text{m}}\text{Tc}$ ]Tc-MDP SPECT/CT in patients with prostate cancer [18]. Tabotta and co-workers determined that the optimum SUV<sub>max</sub> cut-off to define bone metastases in the spine and pelvis on [ $^{99\text{m}}\text{Tc}$ ]Tc-2,3-dicarboxy propane-1,1-diphosphonate (DPD) SPECT/CT was 19.5 [19]. The volume with uptake depends on the VOI. Thus, the definition of the SUV threshold for volumetric analysis is an important issue, and further research is needed to establish a threshold.

The most important factors for generating quantitative SPECT and PET data are the scanner calibration and the reconstruction algorithms that correct for photon attenuation and scattering within the object [5]. Reliable calculation of SUV parameters also

requires an accurate injection dose, injection time, and patient weight [4]. In a study by Arvola et al., the SUV ratios of the lesion were calculated by dividing the lesion SUV by the background bone activity SUV, which can be calculated without scanner calibration or information about the accurate injection dose or patient weight. This is technically easier to achieve than with an SUV [4]. The authors suggested that SPECT SUV ratios could be used to expand the visual analysis of bone SPECT, especially in follow-up studies to decrease inter-observer variability and standardize SPECT results among patients, imaging scanners, and clinical centers [4].

The main limitations of this study are its retrospective, single-center design, small sample size with only prostate cancer patients, and lack of histopathological analysis for bone metastases. In the future, it will be necessary to consider not only prostate cancer but also other cancer types in studies with larger cohorts. Lesions visible only on either SPECT or PET should also be considered in future studies. A threshold for contouring lesion volume was selected by visual inspection to best fit the contour of abnormal uptake. In this method, the lesion boundary may be easily altered by changing the window width/level. However, this method was better than setting a single threshold for contouring small lesions or lesions with a low radiotracer uptake. Some studies have indicated that gradient-based segmentation methods are better than manual- and threshold-contouring methods [20–22]. Since MBV and TBU highly depend on segmentation, i.e., thresholding, further study is required to address the correlation of these volumetric values between SPECT and PET. Defining the threshold for volumetric analysis is an important issue, and further research is needed to establish this step. Because only skeletal lesions visible on both SPECT and PET images were assessed, no data were provided on their relative diagnostic accuracy, such as the differential diagnosis of benign and metastatic bone lesions. In patients with suspected recurrence or progression, the therapeutic circumstances vary. In the future, it may be clinically useful to develop a new method to delineate SPECT based on PET as the gold standard.

## Conclusions

These preliminary results obtained in a limited patient population demonstrate that the SUV- and volume-based parameters are strongly correlated between SPECT/CT and PET/CT for the evaluation of bone metastases in patients with prostate cancer. The SUV parameters in SPECT/CT were significantly lower than those in PET/CT, although the uptake volume in SPECT/CT was significantly higher than that obtained with PET/CT.

## Abbreviations

|         |  |
|---------|--|
| 3D      | Three-dimensional                          |
| DPD     | 2,3-Dicarboxy propane-1,1-diphosphonate    |
| HDP     | Hydroxyethylene                            |
| MBV     | Metabolic bone volume                      |
| MDP     | Methylene diphosphonate                    |
| NaF     | Sodium fluoride                            |
| OSEM    | Ordered-subset expectation–maximization    |
| PET     | Positron emission tomography               |
| SPECT   | Single photon emission computed tomography |
| SUV     | Standardized uptake value                  |
| SUVmax  | Maximum SUV                                |
| SUVmean | Mean SUV                                   |
| SUVpeak | Peak SUV                                   |
| TBU     | Total bone uptake                          |



VOI Volume of interest

### Acknowledgements

Not applicable.

### Author contributions

All the authors contributed to the concept and design of this study. This study was designed by KT and TN. Material preparation, data collection, and analysis were performed by KT, TN, KM, YY, YM, KF, YT, MI, HAO, YT, and NK. The first draft of the manuscript was written by KT and TN and reviewed by YY, MS, and NK. All authors read and approved the final manuscript.

### Funding

No funding was received.

### Availability of data and materials

The data that support the findings of this study are available from the corresponding author on reasonable request.

### Declarations

#### Ethics approval and consent to participate

All procedures performed in this study were conducted in accordance with the ethical standards of the institutional and/or national research committee and with the 1964 Declaration of Helsinki and its later amendments or comparable ethical standards. This study was approved by the Ethics Committee of Kagawa University. The requirement for obtaining informed consent was waived.

#### Consent for publication

Not applicable.

#### Competing interests

The authors declare that they have no competing interests.

Received: 2 October 2022 Accepted: 17 November 2022

Published online: 05 December 2022

### References

1. Abuzalouf S, Dayes I, Lukka H. Baseline staging of newly diagnosed prostate cancer: a summary of the literature. *J Urol*. 2004;171:2122–7.
2. Rigaud J, Tiguert R, Le Normand L, Karam G, Glemain P, Buzelin JM, et al. Prognostic value of bone scan in patients with metastatic prostate cancer treated initially with androgen deprivation therapy. *J Urol*. 2002;168:1423–6.
3. Even-Sapir E, Metser U, Mishani E, Lievshitz G, Lerman H, Leibovitch I. The detection of bone metastases in patients with high-risk prostate cancer:  $^{99m}\text{Tc}$ -MDP planar bone scintigraphy, single- and multi-field-of-view SPECT,  $^{18}\text{F}$ -fluoride PET, and  $^{18}\text{F}$ -fluoride PET/CT. *J Nucl Med*. 2006;47:287–97.
4. Arvola S, Jambor I, Kuisma A, Kempainen J, Kajander S, Seppänen M, et al. Comparison of standardized uptake values between  $^{99m}\text{Tc}$ -HDP SPECT/CT and  $^{18}\text{F}$ -NaF PET/CT in bone metastases of breast and prostate cancer. *EJNMMI Res*. 2019;9:6.
5. Bailey DL, Willowson KP. An evidence-based review of quantitative SPECT imaging and potential clinical applications. *J Nucl Med*. 2013;54:83–9.
6. Bailey DL, Willowson KP. Quantitative SPECT/CT: SPECT joins PET as a quantitative imaging modality. *Eur J Nucl Med Mol Imaging*. 2014;41:S17–25.
7. Cook GJ, Azad G, Padhani AR. Bone imaging in prostate cancer: the evolving roles of nuclear medicine and radiology. *Clin Transl Imaging*. 2016;4:439–47.
8. Jambor I, Kuisma A, Ramadan S, Huovinen R, Sandell M, Kajander S, et al. Prospective evaluation of planar bone scintigraphy, SPECT, SPECT/CT,  $^{18}\text{F}$ -NaF PET/CT and whole body 1.5T MRI, including DWI, for the detection of bone metastases in high risk breast and prostate cancer patients: SKELETA clinical trial. *Acta Oncol*. 2016;55:59–67.
9. Langsteiger W, Heinisch M, Fogelman I. The role of fluorodeoxyglucose,  $^{18}\text{F}$ -dihydroxyphenylalanine,  $^{18}\text{F}$ -choline, and  $^{18}\text{F}$ -fluoride in bone imaging with emphasis on prostate and breast. *Semin Nucl Med*. 2006;36:73–92.
10. Schirrmeyer H, Guhlmann A, Kotzerke J, Santjohanser C, Kühn T, Kreienberg R, et al. Early detection and accurate description of extent of metastatic bone disease in breast cancer with fluoride ion and positron emission tomography. *J Clin Oncol*. 1999;17:2381–9.
11. Yen RF, Chen CY, Cheng MF, Wu YW, Shiau YC, Wu K, et al. The diagnostic and prognostic effectiveness of  $^{18}\text{F}$ -sodium fluoride PET-CT in detecting bone metastases for hepatocellular carcinoma patients. *Nucl Med Commun*. 2010;31:637–45.
12. Araz M, Aras G, Küçük ÖN. The role of  $^{18}\text{F}$ -NaF PET/CT in metastatic bone disease. *J Bone Oncol*. 2015;4:92–7.
13. Cook G Jr, Parker C, Chua S, Johnson B, Aksnes AK, Lewington VJ.  $^{18}\text{F}$ -fluoride PET: changes in uptake as a method to assess response in bone metastases from castrate-resistant prostate cancer patients treated with 223Ra-chloride (Alpharadin). *EJNMMI Res*. 2011;1:4.
14. Wong KK, Pierr M. Dynamic bone imaging with  $^{99m}\text{Tc}$ -labeled diphosphonates and  $^{18}\text{F}$ -NaF: mechanisms and applications. *J Nucl Med*. 2013;54:590–9.

15. Grant FD, Fahey FH, Packard AB, Davis RT, Alavi A, Treves ST. Skeletal PET with  $^{18}\text{F}$ -fluoride: applying new technology to an old tracer. *J Nucl Med*. 2008;49:68–78.
16. Rausch I, Cal-González J, Dapra D, Gallowitsch HJ, Lind P, Beyer T, et al. Performance evaluation of the biograph mCT flow PET/CT system according to the NEMA NU2-2012 standard. *EJNMMI Phys*. 2015;2:26.
17. Dong X, Saripan IM, Mahmud R, Mashohor S, Wang A. Characterization of SIEMENS symbia T SPECT camera in Monte Carlo simulation environment. *Pak J Nuclear Med*. 2018;8:18–26.
18. Umeda T, Koizumi M, Fukai S, Miyaji N, Motegi K, Nakazawa S, et al. Evaluation of bone metastatic burden by bone SPECT/CT in metastatic prostate cancer patients: defining threshold value for total bone uptake and assessment in radium-223 treated patients. *Ann Nucl Med*. 2018;32:105–13.
19. Tabotta F, Jreige M, Schaefer N, Becce F, Prior JO, Nicod LM. Quantitative bone SPECT/CT: high specificity for identification of prostate cancer bone metastases. *BMC Musculoskelet Disord*. 2019;20:619.
20. Rufini V, Collarino A, Calcagni ML, Meduri GM, Fuoco V, Pasciuto T, et al. The role of  $^{18}\text{F}$ -FDG-PET/CT in predicting the histopathological response in locally advanced cervical carcinoma treated by chemo-radiotherapy followed by radical surgery: a prospective study. *Eur J Nucl Med Mol Imaging*. 2020;47:1228–38.
21. Werner-Wasik M, Nelson AD, Choi W, Arai Y, Faulhaber PF, Kang P, et al. What is the best way to contour lung tumors on PET scans? Multiobserver validation of a gradient-based method using a NSCLC digital PET phantom. *Int J Radiat Oncol Biol Phys*. 2012;82:1164–71.
22. Im HJ, Bradshaw T, Solaiyappan M, Cho SY. Current methods to define metabolic tumor volume in positron emission tomography: which one is better? *Nucl Med Mol Imaging*. 2018;52:5–15.

### Publisher's Note

Springer Nature remains neutral with regard to jurisdictional claims in published maps and institutional affiliations.

**Submit your manuscript to a SpringerOpen<sup>®</sup> journal and benefit from:**

- ▶ Convenient online submission
- ▶ Rigorous peer review
- ▶ Open access: articles freely available online
- ▶ High visibility within the field
- ▶ Retaining the copyright to your article

---

Submit your next manuscript at ▶ [springeropen.com](https://www.springeropen.com)

---